Photosynth Res (2015) 125:151–166
DOI 10.1007/s11120-015-0093-1

REGULAR PAPER

Low PSI content limits the photoprotection of PSI and PSII in early growth stages of chlorophyll *b*-deficient wheat mutant lines

Marian Brestic · Marek Zivcak · Kristyna Kunderlikova · Oksana Sytar · Hongbo Shao · Hazem M. Kalaji · Suleyman I. Allakhverdiev

Received: 1 October 2014 / Accepted: 22 January 2015 / Published online: 4 February 2015

Abstract In vivo analyses of electron and proton transport-related processes as well as photoprotective responses were carried out at different stages of growth in chlorophyll *b* (Chl *b*)-deficient mutant lines (ANK-32A and ANK-32B) and wild type (WT) of wheat (*Triticum aestivum* L.). In addition to a high Chl *a*–*b* ratio, ANK mutants had a lower content of photo-oxidizable photosystem I (PSI, P_m), and several parameters indicated a low PSI/PSII ratio. Moreover, simultaneous measurements of Chl fluorescence and P700 indicated a shift of balance between redox poise of the PSII acceptor side and the PSII donor side, with preferential reduction of the plastoquinone pool, resulting in an over reduced PSI acceptor side (high Φ_{NA} values). This was the probable reason for PSI inactivation observed in the ANK mutants, but not in WT. In later growth phases, we observed partial relief of "*chlorina* symptoms," toward WT. Measurements of ΔA_{520} decay confirmed that, in early growth stages, the ANK mutants with low PSI content had a limited capacity to build up the transthylakoid proton gradient (ΔpH) needed to trigger non-photochemical quenching (NPQ) and to regulate the electron transport by cytochrome b_6/f. Later, the increase in the PSI/PSII ratio enabled ANK mutants to reach full NPQ, but neither over reduction of the PSI acceptor side nor PSI photoinactivation due to imbalance between the activity of PSII and PSI was mitigated. Thus, our results support the crucial role of proper regulation of linear electron transport in the protection of PSI against photoinhibition. Moreover, the ANK mutants of wheat showing the dynamic developmental changes in the PSI/PSII ratio are presented here as very useful models for further studies.

M. Brestic · M. Zivcak · K. Kunderlikova · O. Sytar · H. Shao
Department of Plant Physiology, Slovak Agricultural University, Tr. A. Hlinku 2, 949 76 Nitra, Slovak Republic
e-mail: marian.brestic@uniag.sk

M. Zivcak
e-mail: marek.zivcak@uniag.sk

K. Kunderlikova
e-mail: xkunderlikov@is.uniag.sk

O. Sytar
e-mail: o_sytar@ukr.net

O. Sytar
Department of Plant Physiology and Ecology, Taras Shevchenko National University of Kyiv, Volodymyrs'ka St. 64, Kiev 01601, Ukraine

H. Shao
Key Laboratory of Coastal Biology & Bioresources Utilization, Yantai Institute of Coastal Zone Research (YIC), Chinese Academy of Sciences (CAS), Yantai 264003, People's Republic of China

H. M. Kalaji (✉)
Department of Plant Physiology, Faculty of Agriculture and Biology, Warsaw Agricultural University SGGW, Nowoursynowska 159, 02-776 Warsaw, Poland
e-mail: hazem@kalaji.pl

S. I. Allakhverdiev
Institute of Plant Physiology, Russian Academy of Sciences, Botanicheskaya Street 35, Moscow 127276, Russia
e-mail: suleyman.allakhverdiev@gmail.com

S. I. Allakhverdiev
Institute of Basic Biological Problems, Russian Academy of Sciences, Pushchino, Moscow 142290, Russia

S. I. Allakhverdiev
Department of Plant Physiology, Faculty of Biology, M.V. Lomonosov Moscow State University, Leninskie Gory 1-12, Moscow 119991, Russia

Keywords *Chlorina* mutants · Wheat · Non-photochemical quenching · Chlorophyll fluorescence · Transthylakoid proton gradient · PSI photoinhibition

Abbreviations

See Materials and methods section for other symbols representing chlorophyll fluorescence and P700 parameters

A_{CO_2}	CO_2 assimilation rate
Chl	Chlorophyll
ChlF	Chlorophyll *a* fluorescence
Cyt b_6f	Cytochrome b_6f
ECS	Electrochromic bandshift
LED	Light emitting diode
LHC	Light harvesting complex
P700	Primary electron donor of PSI (reduced form)
$P700^+$	Primary electron donor of PSI (oxidized form)
PAR	Photosynthetic active radiation
Pmf	Proton motive force
PQ	Plastoquinone
PSI	Photosystem I
PSII	Photosystem II
Q_A, Q_B	Primary, secondary PSII acceptor
RCs	Reaction centers
ROS	Reactive oxygen species
q_E	pH-dependent energy dissipation
WT	Wild type; the genotype with normal chlorophyll synthesis
ΔA_{520}	Absorbance changes at 520 nm
ΔpH	Transthylakoid pH gradient

Introduction

Studies based on photosynthetic mutants help us know better the flexibility and complementarities of individual photosynthetic mechanisms. The mutants with reductions in chlorophyll *b* (Chl *b*) of a typical yellow–green phenotype, called also 'chlorina' mutants, have been frequently used by many laboratories, especially in the 1980s and 1990s of the twentieth century, thus bringing a significant contribution to photosynthetic research (e.g., Ghirardi and Melis 1988; Krol et al. 1995; Gilmore et al. 1996; Bossmann et al. 1997, and others). Most of these papers aimed at answering the questions of how a plant determines the appropriate amounts of Chl and light harvesting complex (LHC) proteins for its growth environment, what controls the biosynthesis of Chl *a* versus Chl *b*, what determines the choice between the syntheses of reaction centers (RCs) versus LHC molecules under different growth conditions, etc. (Falbel et al. 1996). The mutants with reductions in Chl *b* with reduced photosynthetic unit sizes were classified on the basis of the amount of Chl *b*: i.e., those with a complete lack of Chl *b*, termed Chl *b*-less mutants, and those with reduced Chl *b* content, termed Chl *b*-deficient mutants (Terao et al. 1985; Falbel et al. 1996). In all instances in which the primary lesion of the mutants was determined, the deficiency was found to be due to a partial block in the Chl synthesis pathway (Falbel and Staehelin 1994, 1996).

In addition to modification in antenna and pigment composition, it cannot be forgotten that the depletions of LHCII in *chlorina* mutants usually result in severe imbalances in the relative rates of excitation of photosystem I (PSI) and photosystem II (PSII; Andrews et al. 1995). This frequently results in a lower proportion of PSI compared to PSII. Changes in distribution of both photosystems (PSs) are considered to be a response of the plant to reduce the imbalance in light absorption between PSI and PSII (Terao et al. 1996; Terao and Katoh 1996). An elevated PSII/PSI ratio creates, however, conditions in which another imbalance can be expected between the two PSs with potentially harmful consequences.

Higher plants dispose with some flexibility, thanks to different mechanisms enabling them to dissipate the excess of excitation energy and to ensure the ATP/NADPH output ratio for plant metabolism (Kramer et al. 2003; Kramer and Evans 2011). It is broadly accepted that the key photoprotection process in PSII is non-photochemical quenching (NPQ), by which excess light energy is harmlessly dissipated as heat (Demmig-Adams and Adams 2006). This process is induced by a low thylakoid lumen pH and a high ΔpH which are generated by photosynthetic electron transport under an excess of light and which activate q_E by protonating the protein PsbS (Li et al. 2000) and activating the xanthophyll cycle (Demmig-Adams 1990). The proton gradient in thylakoids is necessary to trigger the ΔpH-dependent regulation of linear electron transport by cytochrome b_6f (Cyt b_6f), which plays a particularly important role also in protecting of PSI against photooxidative damage. Indeed, an over reduction of PSI acceptor side may lead to excessive production of reactive oxygen species (ROS; Schmitt et al. 2014) and PSI photoinhibition (Miyake 2010). It appears that PSI is protected mainly by the activity of cyclic electron flow (Bukhov and Carpentier 2004), which contributes to the buildup of transthylakoid ΔpH (Joliot and Johnson 2011) or it simply removes excessive electrons from the PSI acceptor side, and acts as a dissipative mechanism in PSI (Laisk et al. 2010). The role of cyclic electron flow was shown to be especially important in stress conditions (Golding and Johnson 2003; Zivcak et al. 2013, 2014b). Moreover, the changes in activities of both PSs may also contribute to the regulation

of linear electron transport, especially in stress conditions (Goltsev et al. 2012; Oukarroum et al. 2013; Wang and Chen 2013, etc.).

There are many contentious issues in the field of photoprotective responses, and further research in this area is still needed. The major progress in the last decades has been achieved using different photosynthetic mutants and transgenic plants. Therefore, we believe that the experiments performed on the *chlorina* mutants with expected imbalance in PSI/PSII function may also contribute to progress in understanding the regulation of electron and proton transport as well as photoprotection of both PSs. In fact, there exists an enormous number of Chl-*b*-deficient or Chl *b*-less mutants of different plant species. Many of them, such as *chlorina* f2, have been extensively studied, and their responses to various conditions are well described (Gilmore et al. 1996; Georgieva et al. 2003; Brestic et al. 2008, etc.). In our study, we decided to use the near-isogenic hexaploid lines of bread wheat denoted as ANK-lines. The genetic basis of mutation, molecular and biochemical properties, as well as phenotype of these mutants are well characterized (Watanabe and Koval 2003; Rassadina et al. 2005; Kosuge et al. 2011); however, there is a lack of information on specific photosynthetic responses of these mutants. On the basis of visual observation, it was found that young plants have a very strong and typical chlorina phenotype and slow growth; however, the chlorina phenotype tends to gradually disappear throughout the life cycle. Thus, the mutant lines are able to survive and produce a satisfactory grain yield even in field conditions. Relatively slow and gradual transition from typical *chlorina* toward the wild-type (WT) phenotype makes them particularly interesting for physiological studies. In this paper, we compare the photosynthetic properties and light responses of mutants compared to WT in two different growth phases. We tried to document that mutation strongly affected the PSI/PSII ratio, which influenced the regulation of electron and proton transport as well as the photoprotective responses in mutant plants.

Materials and methods

Plant material and cultivation

The plants of spring wheat (*Triticum aestivum* L.) were used for the experiments. The Chl-*b*-deficient "chlorina" mutants ANK-32A and ANK-32B (hereinafter denoted as ANK mutants) are near-isogenic hexaploid lines containing a *chlorina* mutation of the cn-A1 locus introduced from the *Chlorina-1* (ANK-32A) or from a *chlorina* mutant line of AN-215 (ANK-32B). Mutant plants have yellow-greenish seedlings and grow slowly during the first half of the growth cycle. At the beginning of heading, plant color becomes visually indistinguishable from WT (Mitrofanova 1991; Koval 1997; Watanabe and Koval 2003). As a "wild type" (WT), we used the non-mutant hexaploid wheat genotype Corso with a similar developmental pattern as both ANK mutant lines.

Wheat plants were grown in pots (nine seedlings per pot) with the standard peat substrate. The pots were regularly irrigated and occasionally fertilized using liquid fertilizer with micronutrients. The cultivation and experiment were carried out in a growth chamber with artificial light provided by fluorescent tubes [growing conditions: 10/14 h dark/light at 16/20 °C; photosynthetic active radiation (PAR) at leaf level $\sim$ 300 µmol photons m^{-2} s^{-1}].

Simultaneous measurements of P700 redox state and Chl fluorescence

The state of PSI and PSII photochemistry was measured with a Dual PAM-100 (Walz, Germany) with a ChlF unit and P700 dual wavelength (830/875 nm) unit, as described by Klughammer and Schreiber (1994). Saturation pulses (10,000 µmol photons m^{-2} s^{-1}), intended primarily for the determination of ChlF parameters were used also for the assessment of the P700 parameters. Prior to the measurements, plants were dark adapted for 15 min in a dark box, and for app. 2 min in the measuring head. After the determination of F_0, F_m, and P_m, the light intensity similar to ambient (134 µmol photons m^{-2} s^{-1}) was used to start the photosynthetic processes. After a steady state was reached, a rapid light curve was triggered (light intensities 14, 30, 61, 103, 134, 174, 224, 347, 539, 833, 1036, 1295, 1602, and 1930 µmol photons m^{-2} s^{-1}; 30 s at each light intensity) with saturation pulse and far-red pulse for F'_0 determination after 30 s at each light intensity. For the calculation of the ChlF parameters, the following basic values were used: F, F'—fluorescence emission from dark- or light-adapted leaf, respectively, F_0—minimum fluorescence from dark-adapted leaf (PSII centers open), F_m, F'_m—maximum fluorescence from dark- or light-adapted leaf, respectively (PSII centers closed), F'_0—minimum fluorescence from light-adapted leaf. The ChlF parameters were calculated as follows (Kramer et al. 2004; Baker 2008): the maximum quantum yield of PSII photochemistry, $F_v/F_m = (F_m - F_0)/F_m$; the actual quantum yield (efficiency) of PSII photochemistry, $\Phi_{PSII} = (F_m - F')/F'_m$, NPQ $= (F_m - F'_m)/F'_m$; quantum efficiency of non-regulated energy dissipation in PSII, $\Phi_{NO} = 1/[\text{NPQ} + 1 + q_L(F_m/F_0 - 1)]$; quantum yield of pH-dependent energy dissipation in PSII, $\Phi_{NPQ} = 1 - \Phi_{PSII} - \Phi_{NO}$; and the redox poise of the primary electron acceptor of PSII, Q_A^-/Q_A total $= 1 - q_P = 1 - [(F'_m - F')/(F'_m - F'_0)]$. The fast-relaxing component of NPQ was calculated: $q_E = F_m/F'_m - F_m/F''_m$, where F''_m is the maximum

fluorescence after dark relaxation following the high light period (Thiele et al. 1997).

For the calculation of the P700 parameters, the following basic values were used: P—P700 absorbance at given light intensity, P_m, P'_m—maximum P700 signal measured using saturation light pulse following short far-red pre-illumination in dark- or light-adapted state. The P700 parameters were calculated as follows (Klughammer and Schreiber 1994): effective quantum yield (efficiency) of PSI photochemistry at given PAR, $\Phi_{PSI} = (P'_m - P)/P_m$; oxidation status of PSI donor side, i.e., the fraction of P700 oxidized at given state, $P700^+/P700$ total $= \Phi_{ND} = P/P_m$; reduction status of PSI acceptor side, i.e., the fraction of overall P700 oxidized in a given state by saturation pulse due to a lack of electron acceptors, $\Phi_{NA} = (P_m - P'_m)/P_m$.

Measurements of electrochromic bandshift

Non-invasive measurements of absorbance changes denoted as electrochromic bandshift (ECS) were performed with an light emitting diode (LED)-based spectrophotometer (JTS 10, Biologic, France) following Joliot and Joliot (2002). The difference in exponential decay of the signals measured at 520 nm (ΔA_{520}) and 546 nm ($\Delta A_{520} - \Delta A_{546}$) in first 100 ms was used as a measure of membrane potential [proton motive force (*pmf*)]. Measuring flashes were provided by a white LED filtered at 520 nm. The time resolution of the instrument was 10 µs. Prior to taking measurements, the sample was pre-illuminated by the artificial white light with intensity ~ 300 µmol photons m^{-2} s^{-1} for at least 2 h. Then, the leaf was inserted into the leaf holder, and the red light (630 nm, intensity 950 µmol photons m^{-2} s^{-1}) was applied for 15 min prior to the measurements of ECS decay. After 15 min at given light intensities, the ECS decay was measured at 520 nm by switching off the actinic light. Then, the leaf was pre-illuminated again with the same intensity for 3 min, and the same protocol of ECS decay was measured at 546 nm. Then, the signal measured at 546 nm was subtracted from the record measured at 520 nm, which allowed deconvolution of the ECS signal from the absorption changes associated with the redox changes related to the electron flow, e.g., the Cyt b_6/f complex (Joliot and Joliot 2002). The amplitude of ECS decay normalized to Chl content will be considered as a measure of *pmf*, as described by Sacksteder and Kramer (2000).

Measurements of gas exchange

The photosynthetic rate was measured in steady-state conditions using a gasometer (Ciras2, PP-Systems, UK). The following conditions were maintained within the measuring head: leaf temperature 20 °C, reference CO_2 content 380 ppm, ambient air humidity, and the actinic light provided by LED light unit (1,000 µmol photons m^{-2} s^{-1}).

Determination of photosynthetic pigments

The segments from the mature, fully expanded leaves were homogenized using sea sand, $MgCO_3$, and 100 % acetone and then extracted with 80 % acetone. After 2-min centrifugation at 2,500 rpm, absorbance of the solution was measured by a UV–vis spectrophotometer (Jenway, UK), at 470, 647, and 663 nm, with a correction for scattering measured at 750 nm. The concentrations of Chl *a*, Chl *b*, and carotenoids (Cars) per leaf area unit were determined, using the equations of Lichtenthaler (1987), as described elsewhere (Zivcak et al. 2014a). Six leaves of each genotype were analyzed.

Simultaneous measurements of red and far-red fluorescence

Fluorescence measurements were performed on leaves at room temperature (~ 21 °C) using a multiparametric fluorescence excitation system (Multiplex-3, Force-A, Orsay, France); the system is described in detail by Ghozlen et al. (2010). The fluorescence in red (peak at 685 nm) and far-red (peak at 735 nm) spectral bands excited with red light pulse was recorded simultaneously, and the fluorescence ratio F_{735}/F_{685} was calculated.

Determination of Q_B^- non-reducing centers

The double-hit method (Strasser et al. 2004) was followed for the calculation of Q_B^- non-reducing centers, as described by Mathur et al. (2011). ChlF induction curves were obtained using a Handy-PEA fluorimeter (Hansatech Instruments Ltd., UK). Two fluorescence transients were induced by two subsequent pulses (each 3,500 µmol photons m^{-2} s^{-1} for 1 s). The first pulse (denoted as first hit) was conducted after a dark period long enough to ensure the reopening of all RCs, followed by a second pulse (second hit). The duration of the dark interval between two hits was 500 ms. The relative amount of Q_B-non-reducing centers (B_o) was calculated by the equation: $B_o = [(F_v/F_m) - (F^*_v/F^*_m)]/(F_v/F_m)$, where F_v and F_m were variable fluorescence and maximal fluorescence of first hit, F^*_v, F^*_m were variable fluorescence and maximal fluorescence of second hit.

Data processing and analysis

The measurements of gas exchange, ChlF, and P700 were analyzed from 6 to 10 repeated measurements. The measurements of ECS decay, Q_B-non-reducing PSII RCs, and

simultaneous measurements of red and far-red fluorescence were carried out in at least 10 repetitions. The mean values ± standard errors ($\alpha = 0.05$) are presented here. The statistical significance of differences was assessed using ANOVA followed by the post-hoc Tukey HSD test to identify statistically homogenous groups.

Results

Photosynthetic parameters measured in ANK wheat mutants were compared with WT in both growth phases representing the beginning (second fully developed leaf) and the ending (fifth fully developed leaf) of the experiment (Table 1).

The value of total Chl (Table 1a) was lower in younger plants than in the latter growth stage; the ANK mutants had significantly lower Chl content than WT. As expected, the Chl *a*–*b* ratio was much higher in Chl *b*-deficient mutants; however, the deficit in Chl *b* was partially alleviated in leaves of older plants, but the Chl *a*/*b* ratio was still much higher in ANK than in WT. Similarly, the Car content was lower in mutants compared to WT; however, the Chl/Car ratio was almost two times higher in ANK mutants than in WT.

Steady-state values of gas exchange parameters (Table 1d) indicate a significantly lower CO_2 assimilation rate in ANK mutants in the early growth phase. This difference was not caused by the stomatal effect, as the C_i value was higher in ANK mutants than in WT. In older plants, the net assimilation rates of WT and ANK mutants were similar. The carboxylation efficiency (indicated by A/C_i ratio) remained lower in ANK mutants, whereas the photosynthesis seems to be more limited by diffusion of CO_2 into the leaf in WT, as indicated by much lower C_i, but relatively high A/C_i ratio in the fifth leaf of WT compared to mutants.

The double-hit method consisting of Chl fluorescence records of two subsequent saturation pulses intermitted by a short dark period (see "Materials and methods" section) indicated a higher proportion of Q_B-non-reducing PSII RCs in ANK mutants compared to WT in both growth phases (Table 1c). The leaves of the older plants contained fewer Q_B-non-reducing centers compared to young plants.

To analyze specific light responses of photosynthetic electron and proton transport in leaves of ANK mutants, we performed Chl fluorescence and P700 measurements consisting of basic measurements of F_0, F_m, and P_m values in dark-adapted leaves followed by slow induction at moderate actinic light intensity, light response curve. Then, the leaves were exposed to the single high light intensity to obtain the steady-state values of parameters in the light-adapted state followed by dark recovery to estimate energy-dependent quenching q_E. The basic ChlF and P700 parameters measured in dark-adapted and high light-exposed state are listed in Table 2.

The value P_m from P700 measurements can be interpreted as the maximum photo-oxidizable PSI content (Schreiber et al. 1988). In addition to higher P_m in the later growth stage, we observed significantly higher P_m in WT than in ANK mutants, and hence, the higher content of PSI in WT. Similarly, the ratio of far-red fluorescence (peak at 735 nm) and red fluorescence (peak at 685 nm; Table 1b) suggested a much lower PSI/PSII ratio in ANK mutants. This assumption is based on experimental evidence that contribution of PSI fluorescence on fluorescence signal at

Table 1 Values of photosynthetic parameters measured in two growth phases in WT and ANK mutants

Parameters*	Early growth phase (second leaf)			Late growth phase (fifth leaf)		
	WT	ANK-32A	ANK-32B	WT	ANK-32A	ANK-32B
(a) Photosynthetic pigments in leaves						
Chlorophyll content (mg m^{-2})	243 ± 17^a	55 ± 2^d	57 ± 2^d	419 ± 5^a	109 ± 3^c	108 ± 2^c
Chlorophyll *a*–*b* ratio	3.95 ± 0.06^a	8.17 ± 0.13^c	8.87 ± 0.44^c	3.13 ± 0.13^a	5.07 ± 0.18^b	5.35 ± 0.19^b
Carotenoid content (mg m^{-2})	54 ± 5^b	22 ± 3^c	27 ± 2^c	86 ± 3^a	33 ± 1^c	35 ± 2^c
(b) Simultaneous measurements of far-red and red fluorescence after red-excitation						
F_{735}/F_{685}	3.13 ± 0.48^c	1.15 ± 0.04^b	1.16 ± 0.04^b	3.44 ± 0.46^c	1.69 ± 0.14^a	1.82 ± 0.17^a
(c) Determination of Q_B-non-reducing PSII centers (double-hit method)						
Q_B-non-reducing PSII (rel.u.)	0.36 ± 0.01^b	0.44 ± 0.01^a	0.42 ± 0.01^a	0.26 ± 0.01^c	0.35 ± 0.01^b	0.35 ± 0.01^b
(d) Steady-state CO_2 assimilation records (PAR 1,000 μmol m^{-2} s^{-1}, air CO_2 380 ppm, 20 °C)						
A_{CO_2} (μmol CO_2 m^{-2} s^{-1})	19.5 ± 0.8^a	12.6 ± 0.5^c	13.0 ± 0.3^c	16.4 ± 0.8^b	15.3 ± 0.5^b	15.8 ± 0.7^b
C_i (ppm)	279 ± 3^a	319 ± 5^b	319 ± 5^b	259 ± 12^a	318 ± 8^b	313 ± 4^b
A/C_i ratio	0.07 ± 0.00^a	0.04 ± 0.00^c	0.04 ± 0.00^c	0.06 ± 0.01^a	0.05 ± 0.00^b	0.05 ± 0.00^b

* Mean values ± standard error; small letters indicate statistically homogenous groups (ANOVA, Tukey HSD test, $\alpha = 0.05$)

Table 2 Values of chlorophyll fluorescence and P700 parameters measured in two growth phases in WT and ANK mutants of wheat

Parameters*	Early growth phase (second leaf)			Late growth phase (fifth leaf)		
	WT	ANK-32A	ANK-32B	WT	ANK-32A	ANK-32B
(a) Basic P700 and chlorophyll fluorescence and parameters (measured in dark-adapted samples)						
P_m	0.98 ± 0.08^a	0.32 ± 0.02^c	0.35 ± 0.01^c	1.03 ± 0.11^a	0.42 ± 0.03^b	0.41 ± 0.03^b
F_v/F_m	0.80 ± 0.00^b	0.85 ± 0.00^a	0.84 ± 0.00^a	0.79 ± 0.00^b	0.84 ± 0.00^a	0.83 ± 0.00^a
F_0	0.55 ± 0.02^a	0.26 ± 0.01^d	0.27 ± 0.01^d	0.58 ± 0.01^a	0.34 ± 0.01^c	0.37 ± 0.01^b
F_m	2.86 ± 0.02^a	1.71 ± 0.03^e	1.66 ± 0.05^e	2.71 ± 0.01^b	2.06 ± 0.02^d	2.17 ± 0.01^c
(b) Steady-state values of chlorophyll fluorescence parameters (PAR 1,000 μmol m^{-2} s^{-1})						
Φ_{PSII}	0.25 ± 0.01^a	0.25 ± 0.00^a	0.25 ± 0.01^a	0.19 ± 0.02^b	0.20 ± 0.01^b	0.17 ± 0.02^b
Φ_{NPQ}	0.56 ± 0.00^b	0.44 ± 0.01^c	0.46 ± 0.01^c	0.59 ± 0.01^{ab}	0.64 ± 0.01^a	0.63 ± 0.01^a
Φ_{NO}	0.19 ± 0.00^b	0.31 ± 0.02^a	0.29 ± 0.01^a	0.21 ± 0.01^b	0.19 ± 0.01^b	0.19 ± 0.01^b
NPQ	1.96 ± 0.01^b	1.05 ± 0.01^c	1.12 ± 0.05^c	2.04 ± 0.09^b	2.46 ± 0.09^a	2.41 ± 0.08^a
q_E	1.72 ± 0.02^b	0.73 ± 0.09^c	0.86 ± 0.05^c	1.91 ± 0.08^{ab}	2.19 ± 0.10^a	2.14 ± 0.10^a
(c) Steady-state values of P700 parameters (PAR 1,000 μmol m^{-2} s^{-1})						
Φ_{PSI}	0.44 ± 0.01^a	0.43 ± 0.01^a	0.43 ± 0.03^a	0.3 ± 0.04^b	0.28 ± 0.01^b	0.27 ± 0.03^b
Φ_{ND}	0.46 ± 0.00^b	0.28 ± 0.02^c	0.31 ± 0.03^c	0.58 ± 0.04^a	0.42 ± 0.03^b	0.45 ± 0.02^b
Φ_{NA}	0.10 ± 0.01^b	0.29 ± 0.02^a	0.26 ± 0.04^a	0.12 ± 0.01^b	0.3 ± 0.04^a	0.27 ± 0.03^a

* Mean values ± standard error; small letters indicate statistically homogenous groups (ANOVA, Tukey HSD test, $\alpha = 0.05$)

room temperature peaks between 720 and 735 nm (more than 40 %), while at 685 nm, the PSI contribution is almost four times lower (Franck et al. 2002). Thus, any decrease in PSI fluorescence contribution (due to lower PSI/PSII ratio) will lead to a greater relative decrease of F_{735} than F_{685}, and thus lower F_{735}/F_{685} ratio.

The basic fluorescence parameters measured in the dark-adapted state (Table 2a) indicate much lower F_0 and F_m values in ANK mutants, especially in young seedlings. Interestingly, there was no significant difference in the values of PSII and PSI quantum efficiencies between WT and ANK mutants; however, there was a significant difference between the leaves in both growth phases. Such a difference probably does not reflect a lower linear electron transport rate, but can be caused by a higher leaf absorbance due to higher Chl content and more abundant PSI and PSII. Φ_{PSI} decreased more than Φ_{PSII} from early to late growth phase (Table 2b); this might be mainly due to changes in PSI/PSII ratio and hence, changes in the distribution of absorbed light between PSII and PSI.

Steady-state values of quantum yield of NPQ, as well as NPQ ratio (Table 2b), were much higher in WT compared to ANK mutants in the early growth phase, whereas at the end, it was reversed. A similar trend was also found in values of the fast-relaxing (energy dependent) component of NPQ (q_E); here, it should be pointed that (unlike NPQ) the difference between WT and ANK mutants in later growth phase was not significant. This was caused by a higher contribution of the slow-relaxing component of NPQ (NPQ − q_E) in ANK mutants in both growth phases.

The values of complimentary quantum yields of PSI photochemistry (Table 2c) indicated much lower Φ_{ND}, i.e., lower oxidation status (redox poise) of P700 (donor side limitation of PSI) in ANK mutants compared to WT in both growth phases. Consequently, the values of Φ_{NA} were higher in ANK mutants indicating more reduced acceptor side of PSI (acceptor side limitation of PSI).

In addition to dark-adapted or high light responses, we also examined photosynthetic responses in conditions of graduating light intensities (Fig. 1).

We observed a similar trend in PSI quantum yield in mutants and WT (Fig. 1a, b), but a much steeper initial decrease in PSII quantum yield in ANK mutants (Fig. 1c, d), especially in young plants. The occurrence of transient increase of Φ_{PSI} following after a steep initial decrease caused an increase in the Φ_{PSI}/Φ_{PSII} ratio, and it can be considered as a symptom of start of cyclic electron flow around PSI in moderate light intensities. Such an increase was present in all samples in both growth phases; this might indicate that the cyclic electron flow was triggered in all samples. In this case, the quantum efficiencies were not useful to estimate the rate of cyclic electron flow using the difference in the PSI and PSII transport rates, as the calculations of ETR in ANK mutants may have produced artifacts due to an expected shift in distribution of absorbed light energy between PSI and PSII.

In the early growth phase, the capacity for NPQ in ANK plants was significantly lower, compared to the later growth phase (Fig. 1e, f). In contrary, we found no differences between growth phases in NPQ capacity in WT.

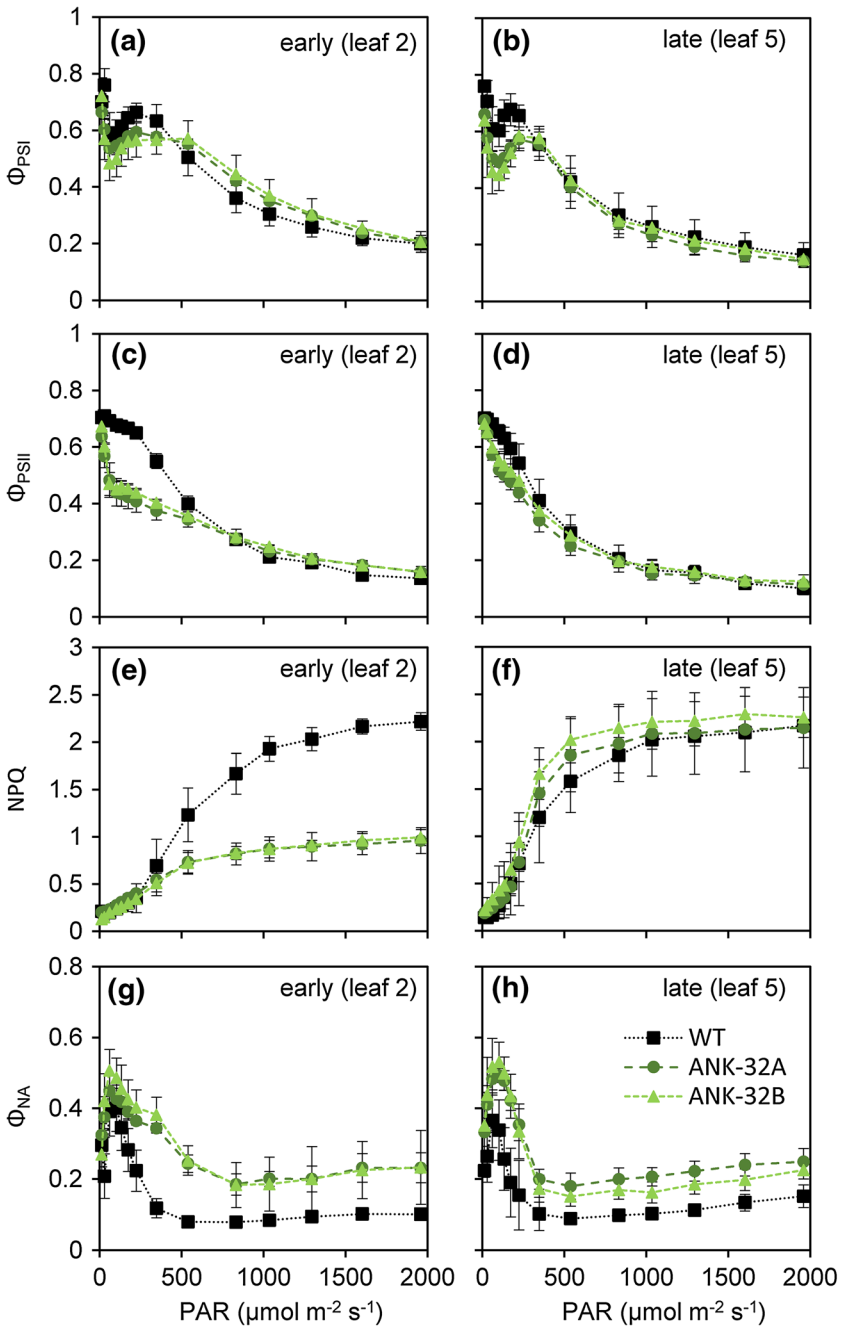

Fig. 1 The values of parameters derived from simultaneous measurements of chlorophyll *a* fluorescence and P700 absorbance in leaves of WT and ANK mutants of wheat, measured in young plants on a fully developed second leaf (*column left* **a**, **c**, **e**, **g**) with records performed later, in fifth leaf (*column right* **b**, **d**, **f**, **h**). **a**, **b** Effective quantum yield of PSII (Φ_{PSII}), **c**, **d** the effective quantum yield of PSI (Φ_{PSI}), **e**, **f** the non-photochemical quenching (NPQ), and **g**, **h** the quantum yield of the PSI non-photochemical quenching caused by the acceptor side limitation, i.e., the fraction of overall P700 not oxidized in a given state (Φ_{NA}). The rapid light curves were obtained after previous induction at moderate light; the duration of each interval with a given light intensity was 30 s (see "Materials and methods" section for details). The average values ± standard errors from six plants are presented

Moreover, the values of NPQ measured after a short period of illumination within light curves in WT were similar to those measured in the steady state, while in ANK mutants, we found significantly higher NPQ in the steady state compared to light curve records. It seems to be associated with the significantly higher slow-relaxing component of NPQ in ANK mutants, as the fast-relaxing component (q_E) quickly reaches the maximum in conditions of excessive light intensity.

A high increase in acceptor side limitation in low light intensities occurred both in WT and ANK mutants (Fig. 1g, h); the maximum Φ_{NA} values were higher in mutants. In WT, it was efficiently decreased in moderate and high light intensities, whereas Φ_{NA} remained relatively high in the ANK mutants, indicating possible over reduction of the PSI acceptor side. Moreover, in the early growth phase of ANK mutants, the decrease in Φ_{NA} with light intensities was relatively slow.

As the result of a different PSI/PSII ratio, we may expect some changes in the balance between processes associated with electron and proton transport on PSI and PSII. For that reason, we analyzed the results obtained

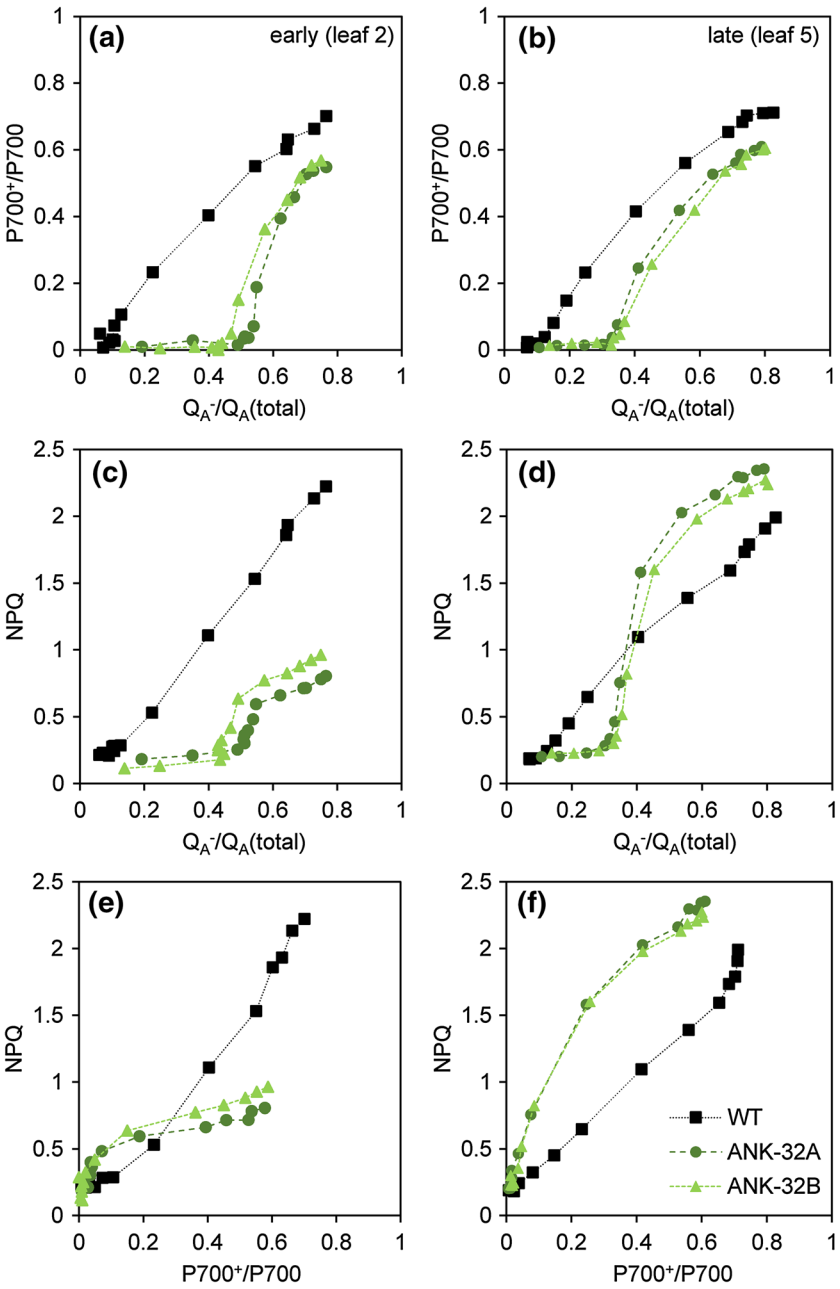

Fig. 2 Relationship between parameters derived from simultaneous measurements of chlorophyll fluorescence and P700 absorbance (Dual-PAM, Walz, Germany) measured in young plants on a fully developed second leaf (*column left* **a**, **c**, **e**) with records performed later, in fifth leaf (*column right* **b**, **d**, **f**). Each point (from *left* to *right*) represents one record from measurements at the graduated intensity of red actinic light (30 s at 15–2,000 µmol m^{-2} s^{-1}) recorded within the light response curve protocol. **a**, **b** relationship between the redox poise of the PSII acceptor side—Q_A^- /Q_A total (derived from ChlF light response curve records as $1 - q_P$) and redox poise of PSI donor side $P700^+$/P700 (calculated from P700 records as parameter Φ_{ND}). **c**, **d** Relationship between redox poise of the PSII acceptor side—Q_A^- /Q_A total and non-photochemical quenching (NPQ derived from ChlF records). **e**, **f** Relationship between $P700^+$/P700 total and non-photochemical quenching (NPQ)

within simultaneous measurements of Chl fluorescence and P700 transmittance on leaves exposed to graduated intensities of red actinic light within the light curves presented above (Fig. 2).

The relationship between the excitation pressure of the PSII acceptor side (Q_A^- /Q_A total) and the oxidation level of the donor side ($P700^+$/P700 total) shows the almost linear relationship in WT in both growth stages (Fig. 2a, b), but we can see the shift of balance in ANK mutants, where the excitation pressure at the beginning increased without oxidation of the PSI donor side. Similar trends were found also when we correlated NPQ with Q_A^- /Q_A total (Fig. 2c, d). NPQ values express mostly an increase in the transthylakoid proton gradient (ΔpH), and we found that the early increase in excitation pressure on the PSII acceptor side in ANK mutants was not associated with an increase in NPQ. On the other hand, we found a simultaneous increase in NPQ with $P700^+$/P700 growth (Fig. 2e, f) until NPQ reached the top of its capacity at the given state. In ANK mutants, increase in NPQ was faster than oxidation of the PSI acceptor side.

Low NPQ as well as slow oxidation of P700 in young plants makes us wonder whether it is caused by a low transthylakoid proton gradient. For this reason, we

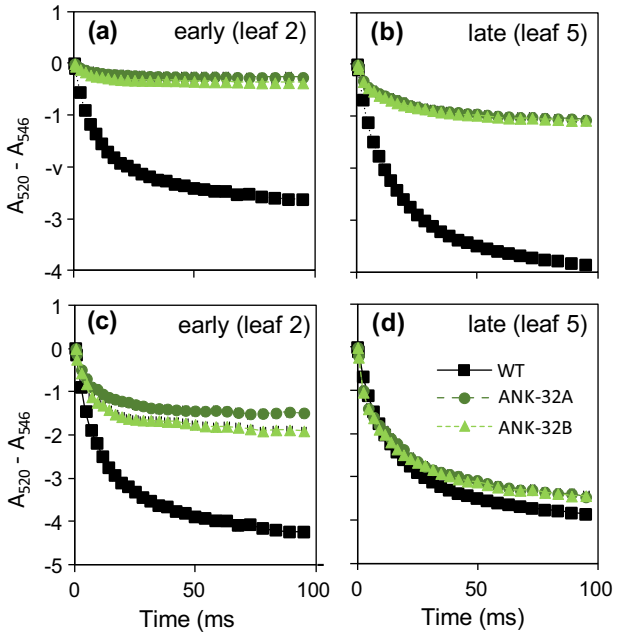

Fig. 3 Decay of the membrane potential upon a light-to-dark transition (ECS decay) followed after 15 min of illumination by strong red actinic light (940 µmol m^{-2} s^{-1}) measured in young plants on a fully developed second leaf (*column left* **a**, **c**) compared with records performed later, in fifth leaf (*column right* **b**, **d**). The *upper graphs* **a**, **b** show the original data (without normalization), the *bottom graphs* **c**, **d** show the data, in which the signal amplitudes were normalized to the leaf chlorophyll content. Average curves of 6–10 ECS records are presented

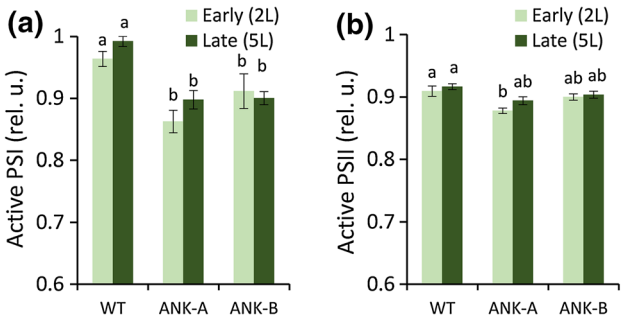

Fig. 4 Portion of active PSI **(a)** and PSII **(b)** measured after high light treatment followed by dark recovery within the applied protocol. Active PSII and PSI units were estimated using F_v/F_m and P_m values, respectively, both measured in dark-relaxed samples before and after high light treatment

compared records of decay of $\Delta A_{520} - \Delta A_{546}$ signal (ECS decay) followed after 15 min of illumination by strong red actinic light (Fig. 3). The amplitude of records from ANK mutants is always much lower than in WT (Fig. 3a). If we normalized the signal on Chl content (Fig. 3b), the amplitude of the decay (*pmf*) recorded in ANK mutants in later growth stages reached or even exceeded *pmf* of WT. In contrast, the amplitude of the ECS signal in young plants (second leaf) was 60–75 % lower compared with WT or later records of ANK mutants. It means that young plants have much lower *pmf* and transthylakoid proton gradient.

During the applied protocols, the leaves were exposed to changing light conditions, as the light intensity was graduated and then kept several minutes at an excessive level, app. four times higher than the intensity at which the plants were grown; moreover, the light periods were interrupted by frequent ($\sim$ 40) saturation pulses and far-red pulses. For this reason, we tested the effect of applied light treatment on PSI and PSII activity after a period of dark relaxation. Analysis of the relative contribution of active PSI RCs using values of P_m before and after high light exposure and dark recovery (Tikkanen et al. 2014) indicated only a negligible level of inactivation of PSI in WT. In contrary, we found app. a 10 % decrease of photooxidizable P700 (P_m), i.e., significant photoinactivation of PSI in ANK mutants in both growth phases (Fig. 4a). Analogical comparison of F_v/F_m values before and after high light treatment and dark recovery indicated the presence of non-relaxed PSII in all samples (Fig. 4b). The values in ANK mutant indicated slightly higher susceptibility of PSII to high light compared to WT; the differences were mostly insignificant.

Discussion

Photosynthetic properties of ANK wheat mutants

Despite being of different origin, the same mutation in two ANK mutants led to almost identical physiological responses, significantly different from WT. The Chl *a*–*b* ratio (Table 1a) ranging from 8.7 in young plants to 5 in older mutant plants was much higher compared with WT (3.9–3.3); thus indicating that the mutant line belongs to the second group—the Chl-deficient mutants. In very young seedlings of these mutant lines, Watanabe and Koval (2003) found a Chl *a*/*b* ratio of around 8 in young seedlings of ANK mutants; this corresponds to our observations. In addition to Chl *b*, the total Chl content (as well as Chl *a*) was strongly reduced in ANK mutants. This is typical for the mutants of the second group, whereas Chl-*b*-lacking mutants have often normal Chl *a* content (Terao et al. 1996). The Car content was much less reduced than the Chl content; hence, the Chl/Car ratio was quite low in ANK mutants.

CO_2 assimilation rate of ANK mutants was relatively high, although in the early growth phase, it was much lower than in WT. In the later growth phase, the CO_2 assimilation was similar to WT. These results correlate with observations that plants of ANK mutants grow slowly in early growth phases, but their growth later is similar to

WT. In general, a high photosynthetic rate of mutants seems to be surprising considering a low level of leaf Chl as the photosynthetic rate per Chl unit is much higher in ANK mutants here; this phenomenon is typical for many *chlorina* mutants (see e.g., Lin et al. 2003; Brestic et al. 2008), and it inevitably brings about the question of efficiency of high Chl content in WT. The low photosynthetic rate of ANK mutants in early growth phases was not caused by closed stomata, as the CO_2 content in mesophyll of ANK leaves (C_i) was much higher. Interestingly, the high C_i value was also found in leaves of mutant plants in the later growth stage, when A_{CO_2} was similar to WT. We suggest that the photosynthetic rate in WT was more limited by CO_2 diffusion to leaf, whereas the ANK mutant had a lower efficiency of carboxylation in both growth phases.

Another specific feature typical for *chlorina* mutants is a lower PSI/PSII ratio as a response to imbalance in light absorption between PSI and PSII. Indeed, antenna sizes of PSII are much more reduced than in PSI (Harrison et al. 1993; Andrews et al. 1995). For example, in *chlorina* mutants of rice, the PSII/PSI ratio was app. 1.3 in WT, but more than 2 in Chl-*b*-deficient mutants (Terao et al. 1996; Terao and Katoh 1996). Without molecular analyses, we were not able to establish the PSI/PSII ratio exactly; some of our results suggest a much lower abundance of PSI compared to PSII. First of all, low P_m values from the P700 measurements (Table 2a) indicate low content of photooxidizable PSI (Grieco et al. 2012). However, this says nothing about the PSI/PSII ratio, as the number of PSII RCs can be decreased as well. On the other hand, the basal fluorescence (F_0) can be considered as a reliable indicator of the PSI/PSII ratio, as the F_0 signal measured by common fluorometers (including PAM-system used here) contains an important contribution by PSI fluorescence (Pfündel et al. 2013). Although it has been previously suggested that F_0 can serve as a measure of Chl content (Strasser et al. 2004), the experimental results clearly document that the F_0 and F_m values were essentially insensitive to the Chl content of the leaf as long as the Chl *a*/*b* ratio remained unaffected. Exceptions are cases where the Chl content is extremely low; even an 80 % loss of the Chl content of sugar beet leaves was not enough to reach the value at which the Chl loss causes a decrease in F_0 or F_m (Dinç et al. 2012). Therefore, the low PSI/PSII ratio has to be responsible for a major part of the F_0 decrease in ANK mutants. Significantly, higher values of F_v/F_m (0.84 in mutants vs. 0.80 in WT) also confirm the higher PSI signal in WT, as its presence causes underestimation of F_v/F_m. Pfündel (1998) proposed a simple method of estimation of the PSI fluorescence contribution to the F_0 value based on the deviation of F_v/F_m from the theoretical value (0.87 for PAM records). It means that the closer the value of F_v/F_m is to 0.87, the lower is the PSI contribution to the measured fluorescence signal. Based on our experimental data, the PSI signal represented app. 36–38 % of F_0 in WT. A very similar value was reported by Franck et al. (2002) for barley (*Hordeum vulgare*). Our estimate of the PSI contribution for ANK mutants ranged from 11–15 % of the F_0 value in young plants, to 15–21 % of F_0 in older plants. Although the low F_0 and F_m values were probably also caused by the low antenna size of PSs (Dinç et al. 2012), in the case of chlorina mutants, the low PSII antenna size is the reason for the low PSI content (Andrews et al. 1995), and therefore, any increase in PSII antenna size has to be associated with an increase in PSI content, both leading to an increase in F_0 and F_m.

To experimentally support the idea of a low PSI/PSII ratio, we measured the fluorescence ratio F_{735}/F_{685} (Table 1). Similar parameters, mostly used in inverse form (F_{685}/F_{730} or similar), were shown to be sensitive to Chl content (Lichtenthaler et al. 1990; Kalaji et al. 2014), but strongly reflect PSII and PSI photochemistry (Agati et al. 1995, 1996; Eullaffroy and Vernet 2003). Relationships between this parameter and P_m resp. F_0 recorded during a whole 6-week period (not only in two growth phases, as presented above) are plotted in Fig. 5. Despite non-linear trends, both P_m and F_0 closely correlated with the F_{735}/F_{685} ratio; these trends strongly support the hypothesis of a low PSI/PSII ratio and its slow increase toward WT values.

Imbalance between PSII and PSI and its functional consequences

It has previously been pointed out that an elevated PSII/PSI ratio creates another imbalance between the two PSs, but little attention has so far been paid to the imbalance reflected by the excessive reduction of plastoquinone (PQ) pool in Chl-*b*-deficient mutants with high PSII/PSI ratios (Terao et al. 1996). This assumption has proven to be valid also for ANK mutant lines of wheat, in which we observed several specific responses clearly associated with altered PSI/PSII ratio.

First, we observed a steep initial decrease in PSII quantum efficiency (Φ_{PSII}) within the light response curve in ANK mutants, which was not balanced by the expected steep increase in NPQ (Fig. 1c). It indicates a fast accumulation of closed PSII RCs due to accumulation of electrons in the PQ pool. On the other hand, the trend of PSI quantum efficiency (Φ_{PSI}) was similar to WT. Imbalances in redox poises of PSII and PSI are more recognizable in the relationship between Q_A^-/Q_A total and $P700^+$/P700 total at graduated light intensities (Fig. 2a, b), which can reliably detect any shift of balance between PSs (Zivcak et al. 2013; Brestic et al. 2014). While in WT, we can see the symmetrical accumulation of Q_A^- in PSII

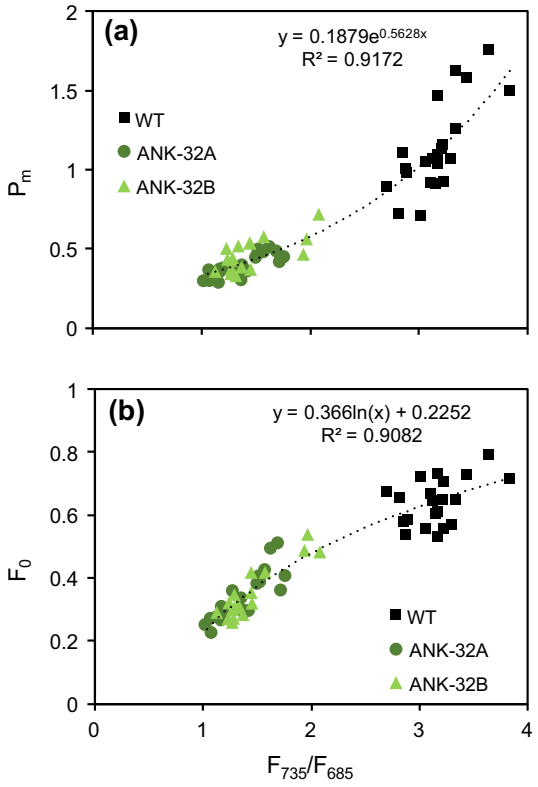

Fig. 5 Relationship between the chlorophyll fluorescence ratio (far-red fluorescence F_{735}–red fluorescence F_{685}) and **a** the maximum photo-oxidizable PSI content (P_m) from P700 measurements (Dual-PAM) and **b** the basal dark-adapted fluorescence level (F_0) from chlorophyll fluorescence records. Measurements were performed on dark-adapted leaves (app. 20 min in dark). *Individual points* represent single measurements realized during the whole period of measurements (app. 1 month); each measurement was performed on the last fully developed leaf (second–fifth leaf of wheat)

acceptor side and $P700^+$ in the donor side of PSI caused by the "bottleneck effect" of Cyt b_6/f (will be discussed below), in ANK mutants, we can see the initial asymmetry when the excitation pressure (expressed by the fraction of closed PSII RCs) quickly increases in PSII without accumulation of oxidized $P700^+$ in PSI. When we plotted Q_A^-/Q_A total against NPQ (Fig. 2c, d), we observed a similar trend. As NPQ can be considered a rough expression of an increase in the transthylakoid proton gradient (ΔpH), the early increase in Q_A^-/Q_A total was not associated with the increase in ΔpH, and hence, it was not caused by ΔpH-dependent regulation of electron transport by Cyt b_6/f, but simply, by the imbalance caused by a low PSI/PSII ratio. This imbalance was partially alleviated, but was still present even in later growth phase.

Another important phenomenon observed in ANK mutants was a low NPQ and q_E capacity in early growth phases, which disappeared later (Table 2b; Fig. 1). Energy-dependent quenching q_E depends on the transthylakoid pH gradient (Briantais et al. 1979) and the presence of pigments of xanthophyll cycle violaxanthin, which is converted to another Car, zeaxanthin (Demmig-Adams 1990). Both protonation and zeaxanthin induce conformational changes in the PSII antenna (Gilmore et al. 1996). Analyses of xanthophyll cycle pigments and fluorescence quenching in the leaves of the mutants indicated that the major LHCII components are not required to facilitate the light-induced quenching associated with zeaxanthin formation (Andrews et al. 1995). Although we did not analyze the xanthophyll cycle pool in ANK mutants, the previous analyses of different *chlorina* mutants indicated usually higher xanthophyll and total concentrations per Chl unit compared with WT (Štroch et al. 2004). We found more Cars per Chl unit, too (Table 1a). On the other hand, our measurements of ECS decay (Fig. 3) indicated a significantly lower *pmf*, and hence, a lower transthylakoid proton gradient (ΔpH) in the early growth phase of ANK mutants, but normal *pmf* (ΔpH) in a later phase. Therefore, we suggest the low *pmf* capacity and not the xanthophyll pool as the main factor that limited q_E in the early growth phase in ANK mutants.

But there remains the question of what caused a limited ability to generate transthylakoid proton gradient. Assuming that F_{735}/F_{685} ratio reflects mostly the PSI/PSII ratio in ANK mutants, the relationship between F_{735}/F_{685} and NPQ capacity (Fig. 6a) indicated a good correlation between the PSI/PSII ratio and NPQ, until the maximum NPQ was reached.

Thus, we may hypothesize that the low number of PSI limited both the capacity to generate sufficient transthylakoid proton gradient and NPQ. Accumulation of H^+ in thylakoid lumen results mostly from processes related to linear or cyclic electron flow, both dependent on PSI activity. On the other hand, H^+ accumulated in the thylakoid lumen serves mostly to drive ATP synthesis (Kramer et al. 2003; Cruz et al. 2005). Thus, the transthylakoid proton gradient is the result of balance between H^+ accumulation and its usage for ATP synthesis. For example, it is well known that in conditions when the Calvin cycle is limited by CO_2 supply (e.g., in conditions of drought stress), ΔpH dramatically increases (Kohzuma et al. 2009; Zivcak et al. 2014b). In contrast, in young ANK mutants, the photosynthetic rate was relatively high, and hence, the demands for ATP were high (especially, when calculated per Chl unit). Therefore, we suggest that in young ANK mutant plants, the PSI content was the limiting factor that caused a limited proton transport and ATP synthesis. The limited ATP synthesis might explain also the low efficiency of CO_2 use (A/C_i ratio) compared to WT or chlorina mutants in latter growth phases (Table 1d). In other words, we suggest that in young ANK mutant plants, there was not only a low PSI/PSII ratio, but also a critically low PSI/ATP-synthase ratio. As soon as the PSI content increased

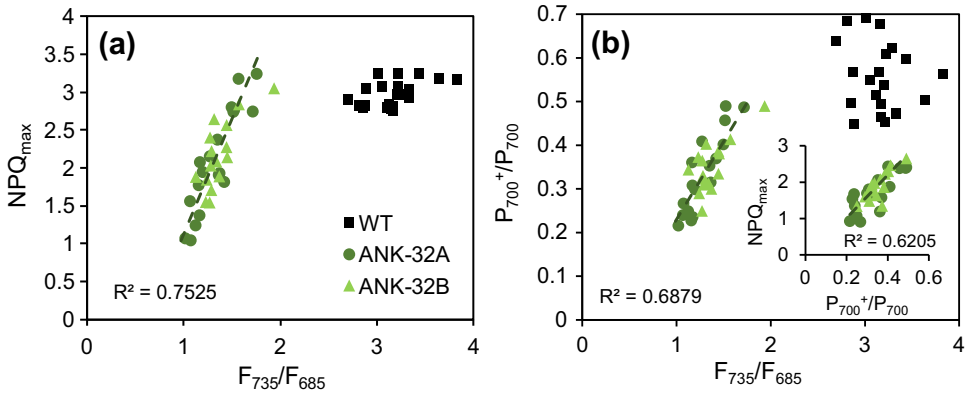

Fig. 6 The relationship between the chlorophyll fluorescence ratio (far-red fluorescence F_{735}–red fluorescence F_{685}) and **a** the maximum value of the non-photochemical quenching (NPQ) parameter measured during high light induction, **b** redox state of PSI electron donor side, and measured in steady state in high light (1000 µmol m^{-2} s^{-1} of light). Small insertion shows relationship between NPQ and redox poise of the PSI donor side. Measurements were performed within protocol consisting of induction curve, light curve, and high light induction. *Individual points* represent single measurements realized during the whole period of measurements (app. 1 month)

above a critical level, *pmf*, NPQ, and A_{CO_2} (A/C_i) also significantly increased.

Of course, there are other possible explanations for low q_E in young ANK mutant plants. Firstly, the essential role of cyclic electron flow in the buildup of the transthylakoid proton gradient is well known (Johnson 2011; Shikanai 2014), and the lack of CET may cause low NPQ. This is the case of the *chlorina* f2 mutant of barley, which was shown to have a low capacity for CET and NPQ (Brestic et al. 2008). However, the shape of the Φ_{PSI} curve (Fig. 1a) and high increase in the Φ_{PSI}/Φ_{PSII} ratio in moderate and high light intensities (not shown here) indicate the presence of CET also in ANK mutant plants in both growth phases. Another possibility can be a lack of some of the proteins necessary for q_E formation, such as PsbS protein (Li et al. 2000). Similarly, the lack of PGR5 prevents the rapid induction of ΔpH-dependent q_E (Foyer et al. 2012).These factors seem to be less probable, as the chlorina mutants have normal levels of PsbS protein (Bossmann et al. 1997), and there is no evidence of changes in function of PGR5 in *chlorina* mutants, as well.

The young ANK mutant plants had relatively high values of Φ_{NO}, i.e., energy loss not provided by NPQ (Kramer et al. 2003), which was, however, not associated with a substantial increase in PSII photoinhibition. A similar observation was made by Ivanov et al. (2008) in *chlorina* f2 mutant. They suggest that this would result in increased probability for an alternative non-radiative $P680^+Q_A^-$ radical pair recombination pathway for energy dissipation within the reaction center of PSII (RC quenching) and that this additional quenching mechanism. Alternatively, Štroch et al. (2004) found that the substantial part of the xanthophyll cycle pigments in *chlorina* f2 mutant of barley was not bound to the remaining pigment–protein complexes and acts as a filter for excitation energy, thereby contributing to the efficient photoprotection under HL. In addition, the role of Q_B-non-reducing RCs of PSII in photoprotection of *chlorina* mutants was also examined (Terao et al. 1996; Yamazaki 2010). In dark-adapted samples, we also identified the higher relative content of Q_B-non-reducing RCs of PSII in ANK mutants (Table 1b). This fraction of PSII RCs is unable to transfer electrons efficiently from the electron acceptor Q_A^- to the secondary electron acceptor Q_B (Melis 1995; Graan and Ort 1986). In such centers, Q_A^- can only be reoxidized by a back reaction with the donor side of PSII (Schanker and Strasser 2005). Q_B-non-reducing differs from Q_B-reducing center in being incapable of reducing the PQ pool. Similar to our results, Terao et al. (1996) found in *chlorina* mutants of rice about 50 % of inactive PSII RCs compared to 20 % in WT. Yamazaki (2010) examined the PSII heterogeneity in *chlorina* mutants in different light conditions. He found that mutant plants regulate their stoichiometry through the adjustment of the contribution of active PSII RCs. The specific function of Q_B-non-reducing centers remains unknown; they might contribute to light absorption or non-photochemical dissipation of absorbed light energy (Terao et al. 1996).

Photoinactivation of PSI

Although PSI is usually thought to be resistant to photoinhibition, it was shown that isolated PSI could be photoinhibited by high light in the absence of PSII activity (Purcell and Carpentier 1994; Rajagopal et al. 2002, 2003). Examples of PSI photoinhibition in low light and low temperature conditions are well known (Sonoike and Terashima 1994; Sonoike 1996); however, the most recent studies (Suorsa et al. 2012; Grieco et al. 2012; Tikkanen et al. 2012, 2014) have clearly demonstrated that PSI may be endangered by photoinhibition if the linear electron flow

is not well regulated even at optimum temperature. Most of the regulation in the thylakoid membrane occurs in order to prevent oxidative damage of PSI (Tikkanen et al. 2012).

The damage of PSI may be a much more serious problem than PSII photoinhibition, as the subsequent recovery of PSI is extremely slow (Sonoike 1996, 2010; Scheller and Haldrup 2005). In this regard, in ANK mutant plants, we found a significant decrease in photo-oxidizable PSI (P_m value) after the measuring procedure (Fig. 4), probably as a result of a permanently increased reduction of PSI acceptor side (indicated by Φ_{NA} parameter). Inactivation of PSI was probably enhanced by frequently applied saturation pulses, as the repetitive illumination with SP-light may lead to severe PSI photoinhibition due to the over reduction of the PSI acceptor side and enhanced production of free hydroxyl radicals (Sejima et al. 2014). In WT, the decrease in P_m was only negligible. This supports the observation that plants are normally well protected against PSI photoinhibition, thanks to the proper regulation of electron transport, and PSI photoinhibition is relatively rare (Sonoike 2010). On the other hand, the mutants with impaired regulation of electron transport (e.g., PGR5 mutant; stn-7 mutant) used to be susceptible to PSI photoinhibition (Suorsa et al. 2012; Grieco et al. 2012; Tikkanen et al. 2012, 2014; Kono et al. 2014).

In all studies, the PSI inactivation was associated with the over reduction of the PSI acceptor side (high Φ_{NA} values). Surplus electrons could lead to photoreduction of molecular oxygen at the acceptor side of PSI and possible formation of harmful amount of hydrogen peroxide (Asada 1999). Addition of scavengers of ROS was reported to protect PSI from photoinhibition (Rajagopal et al. 2005). The studies of PSI photoinactivation have shown that the primary reason of PSI photoinactivation is the hydroxyl radicals produced by reaction between hydrogen peroxide and light-reduced iron–sulfur centers of PSI. They trigger the conformational change in the PSI complex which allows access of a serine-type protease to PsaB (Sonoike et al. 1997). It was clearly demonstrated that photoinactivation of PSI runs only in normal (high) oxygen content in the atmosphere, but not in low oxygen (Sonoike and Terashima 1994; Sejima et al. 2014); this supports the mechanism of photoinhibition of PSI by radicals produced on the PSI acceptor side. Kreslavski et al. (2014) observed maximum production of H_2O_2 app. 30 min after stress conditions were induced; thus the, duration of treatment can be sufficient to observe negative effects on PSI. Chloroplasts cannot fully avoid the production of ROS, and the antioxidant scavenging system for their detoxification has evolved in plant chloroplasts (Asada 1999; Li et al. 2009). Anyway, the high reduction level of PSI acceptors can lead to the production of hydroxyl radicals, which exceeds the capacity of the antioxidant system.

To avoid this, the system is regulated to prevent over reduction of the PSI acceptor side by several mechanisms. Activation of cyclic electron transport has been considered to act as a safety valve (Munekage et al. 2004; Rumeau et al. 2007; Johnson 2011). But the importance of this mechanism for PSI photoprotection in a fluctuating light environment has been questioned (Suorsa et al. 2012). The major role in preventing excessive PSI reduction is played by the efficient regulation of linear electron transport (Joliot and Johnson 2011). As we mentioned before, the illumination of AL induces ΔpH across thylakoid membranes by both linear and cyclic electron flow, which results in the oxidation of P700 (observed as the increase in Φ_{ND}, i.e., $P700^+$/P700). The acidification of the luminal side of thylakoid membranes decreases the oxidation activity of plastoquinol by the site Cyt b_6/f complex (Tikkanen et al. 2012) and induces an increase in NPQ (Niyogi 2000). Under these conditions, the electron flux from PSII to PSI is down-regulated, leading to a decrease in the reduction level of the PSI acceptor side (Φ_{NA}). The light response curve of Φ_{NA} values (Fig. 1g, h) confirms this mechanism, as the Φ_{NA} decreased as soon as the NPQ increase was triggered. Evidently, in the young ANK plants with limited transthylakoid proton gradient (Fig. 1g), the decrease in Φ_{NA} was much slower compared to WT or mutants in the latter growth phase (Fig. 1h).

According to Miyake et al. (2005), the PSI photoinhibition is avoided when the photooxidation rate of P700 in PSI exceeds the reduction rate of P700. Φ_{ND} represents a measure of P700 photooxidation. Similar to NPQ, the Φ_{ND} increased when the PSI/PSII ratio increased as a result of an increase in transthylakoid proton gradient during ontogenesis of ANK mutants (Fig. 6b). However, despite the very efficient decrease in Φ_{NA} in the later growth phase of ANK mutants, the high light value of Φ_{NA} was significantly higher than in WT in both growth phases. Based on this, we suggest that even the properly functioning regulation of linear electron flow was not sufficient to prevent a high reduction in the PSI acceptor side, when the PSI/PSII ratio was too low. The increase in maximum Φ_{NA} before the onset of ΔpH-dependent down-regulation of linear electron flow (peak of Φ_{NA} in Fig. 1g, h) in later growth phase can be caused by an increase in the PSII antenna size, leading to more electrons released by PSII into the electron transport chain. Thus, the increased capacity to down-regulate Φ_{NA} in the later growth phase (compared to young seedlings) was not sufficient to reach values of Φ_{NA} typical for WT in high light conditions. The similar Φ_{NA} in early and late growth phase corresponded with similar levels of PSI photoinactivation in ANK mutants. In this respect, we can conclude that the imbalance between the number of PSI and PSII sets conditions for the higher susceptibility of PSI to photoinhibition. This corresponds with the findings of

Grieco et al. (2012) that the lower the amount of PSI is, the higher is the intersystem redox unbalance.

In past, authors have expected enhanced PSII photoinhibition due to an imbalance between PSI and PSII in *chlorina* mutants (Andrews et al. 1995; Terao et al. 1996). However, PSII photoinhibition has not been considered as an unavoidable and harmful reaction, but the PSII photoinhibition-repair cycle is thought to be an active regulatory component of the photosynthetic electron transfer reactions (Sonoike 1996; Tikkanen et al. 2014). PSII turnover is dynamically regulated according to the energetic state of the thylakoid membrane, allowing the balancing of the amount of active PSII with the capacity of PSI electron acceptors (Murata et al. 2012). Thus, it represents a mechanism of photoprotection for the entire photosynthetic electron transport chain, including PSI (Tikkanen et al. 2012). Our study indirectly supports these findings and we suggest the PSI and not PSII is the main target of damage caused by a low PSI/PSII ratio.

Concluding all, the results of our study suggest that a low PSI–PSII ratio strongly affects the photoprotective responses in Chl-*b*-deficient ANK mutants of wheat. In young mutant seedlings, the low transthylakoid proton gradient was limiting for NPQ (q_E) and ΔpH-dependent regulation of the linear electron flow. Along with the increase in PSI content (PSI/PSII ratio), the capacity to generate q_E increased as a result of a rise in transthylakoid ΔpH. The imbalance between the accumulation of electrons in the PQ pool and the rate of P700 oxidation led to the more reduced acceptor side of PSI, which resulted in small, but significant PSI inactivation in ANK mutants in both growth phases. Thus, we suggest that the low PSI/PSII ratio sets conditions for PSI photoinhibition, especially in fluctuating light. The Chl-*b*-deficient wheat mutant lines—thanks to their slow changes in composition of antenna complexes with their functional consequences—represent a useful tool for research into the regulation of electron and proton transport and photoprotection. We may expect that further studies using these mutants in conditions of fluctuating light or stress may contribute significantly to the recent knowledge in this field.

Acknowledgments This work was supported by the European Community under the Project No. 26220220180: "Construction of the 'AgroBioTech' Research Centre." SIA was supported by Grants from the Russian Foundation for Basic Research, and by Molecular and Cell Biology Programs of the Russian Academy of Sciences.

References

Agati G, Mazzinghi P, Fusi F, Ambrosini I (1995) The F685F730 chlorophyll fluorescence ratio as a tool in plant physiology: response to physiological and environmental factors. J Plant Physiol 145:228–238

Agati G, Mazzinghi P, Lipucci di Paola M, Cecchi G, Fusi F (1996) The F685/F730 chlorophyll fluorescence ratio as indicator of chilling stress in plants. J Plant Physiol 148:384–390

Andrews JR, Fryer MJ, Baker NR (1995) Consequences of LHC II deficiency for photosynthetic regulation in chlorina mutants of barley. Photosynth Res 44:81–91

Asada K (1999) The water–water cycle in chloroplasts: scavenging of active oxygens and dissipation of excess photons. Annu Rev Plant Physiol 50:601–639

Baker NR (2008) Chlorophyll fluorescence: a probe of photosynthesis *in vivo*. Annu Rev Plant Biol 59:89–113

Bossmann B, Knoetzel J, Jansson S (1997) Screening of chlorina mutants of barley (*Hordeum vulgare* L.) with antibodies against light-harvesting proteins of PS I and PS II: absence of specific antenna proteins. Photosynth Res 52:127–136

Brestic M, Zivcak M, Olsovska K, Repkova J (2008) Functional study of PS II and PS I energy use and dissipation mechanisms in barley wild type and chlorina mutants under high light conditions. In: Photosynthesis. Energy from the sun. Springer, Dordrecht, pp 1407–1411

Brestic M, Zivcak M, Olsovska K, Shao HB, Kalaji HM, Allakhverdiev SI (2014) Reduced glutamine synthetase activity plays a role in control of photosynthetic responses to high light in barley leaves. Plant Physiol Biochem 81:74–83

Briantais JM, Vernotte C, Picaud M, Krause GH (1979) A quantitative study of the slow decline of chlorophyll *a* fluorescence in isolated chloroplasts. Biochim Biophys Acta 548:128–138

Bukhov N, Carpentier R (2004) Alternative photosystem I-driven electron transport routes: mechanisms and functions. Photosynth Res 82:17–33

Cruz JA, Avenson TJ, Kanazawa A, Takizawa K, Edwards GE, Kramer DM (2005) Plasticity in light reactions of photosynthesis for energy production and photoprotection. J Exp Bot 56:395–406

Demmig-Adams B (1990) Carotenoids and photoprotection in plants: a role for the xanthophyll zeaxanthin. Biochim Biophys Acta 1020:1–24

Demmig-Adams B, Adams WW (2006) Photoprotection in an ecological context: the remarkable complexity of thermal energy dissipation. N Phytol 172:11–21

Dinç E, Ceppi MG, Tóth SZ, Bottka S, Schansker G (2012) The chl *a* fluorescence intensity is remarkably insensitive to changes in the chlorophyll content of the leaf as long as the chl *a*/*b* ratio remains unaffected. Biochim Biophys Acta 1817:770–779

Eullaffroy P, Vernet G (2003) The F684/F735 chlorophyll fluorescence ratio: a potential tool for rapid detection and determination of herbicide phytotoxicity in algae. Water Res 37:1983–1990

Falbel TG, Staehelin LA (1994) Characterization of a family of chlorophyll-deficient wheat and barley mutants with defects in the Mg-insertion step of chlorophyll biosynthesis. Plant Physiol 104:639–648

Falbel TG, Staehelin LA (1996) Partial blocks in the early steps of the chlorophyll synthesis pathway: a common feature of chlorophyll *b*-deficient mutants. Physiol Plant 97:311–320

Falbel TG, Meehl JB, Staehelin LA (1996) Severity of mutant phenotype in a series of chlorophyll-deficient wheat mutants depends on light intensity and the severity of the block in chlorophyll synthesis. Plant Physiol 112:821–832

Foyer CH, Neukermans J, Queval G, Noctor G, Harbinson J (2012) Photosynthetic control of electron transport and the regulation of gene expression. J Exp Bot 63:1637–1661

Franck F, Juneau P, Popovic R (2002) Resolution of the Photosystem I and Photosystem II contributions to chlorophyll fluorescence of intact leaves at room temperature. Biochim Biophys Acta 1556:239–246

Georgieva K, Fedina I, Maslenkova L, Peeva V (2003) Response of chlorina barley mutants to heat stress under low and high light. Funct Plant Biol 30:515–524

Ghirardi ML, Melis A (1988) Chlorophyll *b* deficiency in soybean mutants. I. Effects on photosystem stoichiometry and chlorophyll antenna size. Biochim Biophys Acta 932:130–137

Ghozlen NB, Cerovic ZG, Germain C, Latouche G, Toutain S (2010) Non-destructive optical monitoring of grape maturation by proximal sensing. Sensors 10:10040–10068

Gilmore AM, Hazlett TL, Debrunner PG (1996) Photosystem II chlorophyll *a* fluorescence lifetimes and intensity are independent of the antenna size differences between barley wild-type and chlorina mutants: photochemical quenching and xanthophyll cycle-dependent nonphotochemical quenching of fluorescence. Photosynth Res 48:171–187

Golding AJ, Johnson GN (2003) Down-regulation of linear and activation of cyclic electron transport during drought. Planta 218:107–114

Goltsev V, Zaharieva I, Chernev P, Kouzmanova M, Kalaji MH, Yordanov I, Krasteva V, Alexandrov V, Stefanov D, Allakhverdiev SI, Strasser RJ (2012) Drought-induced modifications of photosynthetic electron transport in intact leaves: analysis and use of neural networks as a tool for a rapid non-invasive estimation. Biochim Biophys Acta 1817:1490–1498

Graan T, Ort DR (1986) Detection of oxygen-evolving photosystem II centers inactive in plastoquinone reduction. Biochim Biophys Acta 852:320–330

Grieco M, Tikkanen M, Paakkarinen V, Kangasjärvi S, Aro EM (2012) Steady-state phosphorylation of light-harvesting complex II proteins preserves Photosystem I under fluctuating white light. Plant Physiol 160:1896–1910

Harrison MA, Nemson JA, Melis A (1993) Assembly and composition of the chlorophyll *a–b* light-harvesting complex of barley (*Hordeum vulgare* L.): immunochemical analysis of chlorophyll bless and chlorophyll *b*-deficient mutants. Photosynth Res 38:141–151

Ivanov AG, Krol M, Zeinalov Y, Huner NPA, Sane PV (2008) The lack of LHCII proteins modulates excitation energy partitioning and PSII charge recombination in Chlorina F2 mutant of barley. Physiol Mol Biol Plants 14:205–215

Johnson GN (2011) Physiology of PSI cyclic electron transport in higher plants. Biochim Biophys Acta 1807:384–389

Joliot P, Johnson GN (2011) Regulation of cyclic and linear electron flow in higher plants. Proc Natl Acad Sci USA 108:13317–13322

Joliot P, Joliot A (2002) Cyclic electron transfer in plant leaf. Proc Natl Acad Sci USA 99:10209–10214

Kalaji HM, Schansker G, Ladle RJ, Goltsev V, Bosa K, Allakhverdiev SI et al (2014) Frequently asked questions about in vivo chlorophyll fluorescence: practical issues. Photosynth Res 122:121–158

Klughammer C, Schreiber U (1994) Saturation pulse method for assessment of energy conversion in PS I. Planta 192:261–268

Kohzuma K, Cruz JA, Akashi K, Munekage YN, Hoshiyasu S, Kramer DM, Yokota A (2009) The long-term responses of the photosynthetic proton circuit to drought. Plant, Cell Environ 32:209–219

Kono M, Noguchi K, Terashima I (2014) Roles of the cyclic electron flow around PSI (CEF-PSI) and O_2-dependent alternative pathways in regulation of the photosynthetic electron flow in short-term fluctuating light in *Arabidopsis thaliana*. Plant Cell Physiol 55:990–1004

Kosuge K, Watanabe N, Kuboyama T (2011) Comparative genetic mapping of the chlorina mutant genes in genus *Triticum*. Euphytica 179:257–263

Koval SF (1997) The catalogue of near-isogenic lines of Novosibirskaya 67 common wheat and principles of their use in experiments. Russ J Genet 33:995–1000

Kramer DM, Evans JR (2011) The importance of energy balance in improving photosynthetic productivity. Plant Physiol 155:70–78

Kramer DM, Cruz JA, Kanazawa A (2003) Balancing the central roles of the thylakoid proton gradient. Trends Plant Sci 8:27–32

Kramer DM, Johnson G, Edwards GE, Kiirats O (2004) New fluorescence parameters for the determination of QA redox state and excitation energy fluxes. Photosynth Res 79:209–218

Kreslavski VD, Lankin AV, Vasilyeva GK, Luybimov VY, Semenova GN, Schmitt F-J, Friedrich T, Allakhverdiev SI (2014) Effects of polyaromatic hydrocarbons on photosystem II activity in pea leaves. Plant Physiol Biochem 81:135–142

Krol M, Spangfort MD, Huner NP, Oquist G, Gustafsson P, Jansson S (1995) Chlorophyll *a*/*b*-binding proteins, pigment conversions, and early light-induced proteins in a chlorophyll *b*-less barley mutant. Plant Physiol 107:873–883

Laisk A, Talts E, Oja V, Eichelmann H, Peterson RB (2010) Fast cyclic electron transport around photosystem I in leaves under far-red light: a proton-uncoupled pathway? Photosynth Res 103:79–95

Li XP, Björkman O, Shih C, Grossman AR, Rosenquist M, Jansson S, Niyogi KK (2000) A pigment-binding protein essential for regulation of photosynthetic light harvesting. Nature 403:391–395

Li Z, Wakao S, Fischer BB, Niyogi KK (2009) Sensing and responding to excess light. Annu Rev Plant Biol 60:239–260

Lichtenthaler HL (1987) Chlorophyll and carotenoids: pigments of photosynthetic biomembranes. Method Enzymol 148:350–382

Lichtenthaler HK, Hak R, Rinderle U (1990) The chlorophyll fluorescence ratio F690/F730 in leaves of different chlorophyll content. Photosynth Res 25:295–298

Lin ZF, Peng CL, Lin GZ, Ou ZY, Yang CW, Zhang JL (2003) Photosynthetic characteristics of two new chlorophyll *b*-less rice mutants. Photosynthetica 41:61–67

Mathur S, Allakhverdiev SI, Jajoo A (2011) Analysis of high temperature stress on the dynamics of antenna size and reducing side heterogeneity of Photosystem II in wheat leaves (*Triticum aestivum*). Biochim Biophys Acta 1807:22–29

Melis A (1995) Functional properties of PS IIβ in spinach chloroplasts. Biochim Biophys Acta 808:334–342

Mitrofanova OP (1991) Creation of the bank of soft wheat marker genes. 1. Analysis of chlorophyll mutations. In: Koval SF (ed) Near-isogenic lines of cultivated species. ICG SO AN SSSR, Novosibirsk, pp 47–57 (in Russian)

Miyake C (2010) Alternative electron flows (water–water cycle and cyclic electron flow around PSI) in photosynthesis: molecular mechanisms and physiological functions. Plant Cell Physiol 51:1951–1963

Miyake C, Miyata M, Shinzaki Y, Tomizawa KI (2005) CO_2 response of cyclic electron flow around PSI (CEF-PSI) in tobacco leaves—relative electron fluxes through PSI and PSII determine the magnitude of non-photochemical quenching (NPQ) of Chl fluorescence. Plant Cell Physiol 46:629–637

Munekage Y, Hashimoto M, Miyake C, Tomizawa KI, Endo T, Tasaka M, Shikanai T (2004) Cyclic electron flow around photosystem I is essential for photosynthesis. Nature 429:579–582

Murata N, Allakhverdiev SI, Nishiyama Y (2012) The mechanism of photoinhibition in vivo: re-evaluation of the roles of catalase, alpha-tocopherol, non-photochemical quenching, and electron transport. Biochim Biophys Acta 1817:1127–1133

Niyogi KK (2000) Safety valves for photosynthesis. Curr Opin Plant Biol 3:455–460

Oukarroum A, Goltsev V, Strasser RJ (2013) Temperature effects on pea plants probed by simultaneous measurements of the kinetics of prompt fluorescence, delayed fluorescence and modulated 820 nm reflection. PLoS ONE 8:e59433

Pfündel EE (1998) Estimating the contribution of photosystem I to total leaf chlorophyll fluorescence. Photosynth Res 56:185–195

Pfündel EE, Klughammer C, Meister A, Cerovic ZG (2013) Deriving fluorometer-specific values of relative PSI fluorescence intensity from quenching of F0 fluorescence in leaves of *Arabidopsis thaliana* and *Zea mays*. Photosynth Res 114:189–206

Purcell M, Carpentier R (1994) Homogeneous photobleaching of chlorophyll holochromes in a photosystem I reaction center complex. Photochem Photobiol 59:215–218

Rajagopal S, Bukhov NG, Carpentier R (2002) Changes in the structure of chlorophyll–protein complexes and excitation energy transfer during photoinhibitory treatment of isolated photosystem I submembrane particles. J Photochem Photobiol, B 62:194–200

Rajagopal S, Bukhov NG, Carpentier R (2003) Photoinhibitory light-induced changes in the composition of chlorophyll–protein complexes and photochemical activity in photosystem-I submembrane fractions. Photochem Photobiol 77:284–291

Rajagopal S, Joly D, Gauthier A, Beauregard M, Carpentier R (2005) Protective effect of active oxygen scavengers on protein degradation and photochemical function in photosystem I submembrane fractions during light stress. FEBS J 272:892–902

Rassadina VV, Averina NG, Koval SF (2005) Disturbance of chlorophyll formation at the level of 5-aminolevulinic acid and Mg-containing porphyrin synthesis in isogenic lines of spring wheat (*Triticum aestivum* L.) marked with genes cn-A1 and cn-D1. Dokl Biol Sci 405:472–473

Rumeau D, Peltier G, Cournac L (2007) Chlororespiration and cyclic electron flow around PSI during photosynthesis and plant stress response. Plant, Cell Environ 30:1041–1051

Sacksteder CA, Kramer DM (2000) Dark-interval relaxation kinetics (DIRK) of absorbance changes as a quantitative probe of steady-state electron transfer. Photosynth Res 66:145–158

Schanker G, Strasser RJ (2005) Quantification of non-QB-reducing centers in leaves using a far-red pre-illumination. Photosynth Res 84:145–151

Scheller HV, Haldrup A (2005) Photoinhibition of photosystem I. Planta 221:5–8

Schmitt F-J, Renger G, Friedrich T, Kreslavski VD, Zharmukhamedov SK, Los DA, Kuznetsov VV, Allakhverdiev SI (2014) Reactive oxygen species: re-evaluation of generation, monitoring and role in stress-signalling in phototrophic organisms. Biochim Biophys Acta 1837:835–848

Schreiber U, Klughammer C, Neubauer C (1988) Measuring P700 absorbance changes around 830 nm with a new type of pulse modulation system. Z Naturforsch C 43:686–698

Sejima T, Takagi D, Fukayama H, Makino A, Miyake C (2014) Repetitive short-pulse light mainly inactivates photosystem I in sunflower leaves. Plant Cell Physiol 55:1184–1193

Shikanai T (2014) Central role of cyclic electron transport around photosystem I in the regulation of photosynthesis. Curr Opin Biotechnol 26:25–30

Sonoike K (1996) Photoinhibition of photosystem I: its physiological significance in the chilling sensitivity of plants. Plant Cell Physiol 37:239–247

Sonoike K (2010) Photoinhibition of photosystem I. Physiol Plant 142:56–64

Sonoike K, Terashima I (1994) Mechanism of photosystem-I photoinhibition in leaves of *Cucumis sativus* L. Planta 194:287–293

Sonoike K, Kamo M, Hihara Y, Hiyama T, Enami I (1997) The mechanism of the degradation of PsaB gene product, one of the photosynthetic reaction centre subunits of photosystem I, upon photoinhibition. Photosynth Res 53:55–63

Strasser RJ, Tsimilli-Michael M, Srivastava A (2004) Analysis of chlorophyll *a* fluorescence transient. In: Papageorgiou G, Govindjee (eds) Advances in photosynthesis and respiration: chlorophyll *a* fluorescence: a signature of photosynthesis. Springer, Dordrecht, pp 321–362

Štroch M, Čajánek M, Kalina J, Špunda V (2004) Regulation of the excitation energy utilization in the photosynthetic apparatus of chlorina f2 barley mutant grown under different irradiances. J Photochem Photobiol, B 75:41–50

Suorsa M, Jarvi S, Grieco M, Nurmi M, Pietrzykowska M, Rantala M, Kangasjarvi S, Paakkarinen V, Tikkanen M, Jansson S, Aro EM (2012) Proton gradient regulation5 is essential for proper acclimation of *Arabidopsis* photosystem I to naturally and artificially fluctuating light conditions. Plant Cell 24:2934–2948

Terao T, Katoh S (1996) Antenna sizes of photosystem I and photosystem II in chlorophyll *b*-deficient mutants of rice. Evidence for an antenna function of photosystem II centers that are inactive in electron transport. Plant Cell Physiol 37:307–312

Terao T, Yamashita A, Katoh S (1985) Chlorophyll *b*-deficient mutants of rice I. Absorption and fluorescence spectra and chlorophyll *a*/*b* ratios. Plant Cell Physiol 26:1361–1367

Terao T, Sonoike K, Yamazaki JY, Kamimura Y, Katoh S (1996) Stoichiometries of photosystem I and photosystem II in rice mutants differently deficient in chlorophyll *b*. Plant Cell Physiol 37:299–306

Thiele A, Winter K, Krause GH (1997) Low inactivation of D1 protein of photosystem II in young canopy leaves of *Anacardium excelsum* under high-light stress. J Plant Physiol 151:286–292

Tikkanen M, Grieco M, Nurmi M, Rantala M, Suorsa M, Aro EM (2012) Regulation of the photosynthetic apparatus under fluctuating growth light. Philos T R Soc B 367:3486–3493

Tikkanen M, Mekala NR, Aro EM (2014) Photosystem II photoinhibition-repair cycle protects Photosystem I from irreversible damage. Biochim Biophys Acta 1837:210–215

Wang LF, Chen YY (2013) Characterization of a wide leaf mutant of rice (*Oryza sativa* L.) with high yield potential in field. Pak J Bot 45:921–926

Watanabe N, Koval SF (2003) Mapping of chlorina mutant genes on the long arm of homoeologous group 7 chromosomes in common wheat with partial deletion lines. Euphytica 129:259–265

Yamazaki J (2010) Changes in the photosynthetic characteristics and photosystem stoichiometries in wild-type and Chl *b*-deficient mutant rice seedlings under various irradiances. Photosynthetica 48:521–529

Zivcak M, Brestic M, Balatová Z, Drevenaková P, Olsovska K, Kalaji HM, Allakhverdiev SI (2013) Photosynthetic electron transport and specific photoprotective responses in wheat leaves under drought stress. Photosynth Res 117:529–546

Zivcak M, Brestic M, Kalaji HM, Govindjee (2014a) Photosynthetic responses of sun- and shade-grown barley leaves to high light: is the lower PSII connectivity in shade leaves associated with protection against excess of light? Photosynth Res 119:339–354

Zivcak M, Kalaji HM, Shao HB, Olšovská K, Brestič M (2014b) Photosynthetic proton and electron transport in wheat leaves under prolonged moderate drought stress. J Photochem Photobiol, B 137:107–115